Post-Cracking Behaviour of Steel Fibre Reinforced Concrete (RILEM Recommendations)

J.A.O.Barros
Assistant Prof., Dep. of Civil Eng., School of Eng., Univ. of Minho, Campus de Azurém, 4810 058 Guimarães, Portugal

J.A.B. Antunes, V.M.C.F. Cunha, A.F. Ribeiro
Researchers, Dep. of Civil Eng., School of Eng., Univ. of Minho, Campus de Azurém, 4810 058 Guimarães, Portugal

Summary

Recently, RILEM TC 162-TDF Committee has proposed a specimen configuration, test procedures and flexural tensile strength parameters to characterize the post-cracking behaviour of the steel fibre reinforced concrete (SFRC). The approach proposed by RILEM is still yet under discussion, mainly, the ability of the flexural tensile strength parameters to simulate the post-cracking behaviour of the SFRC on the verifications to the ultimate and serviceability limit states. Taking the recommendations of the RILEM, the influence of the fibre content, the concrete age, and the percentage of cement replaced by fly ash on the bending behaviour of the SFRC was analysed in the present work. The influence of the fibre distribution on the fracture surface of the specimens was also considered. The experimental campaign was carried out with a cost competitive SFRC developed for industrial pavements. Bending tests with concrete specimens reinforced with conventional bars and steel fibres were also performed for developing a reinforcement system adjusted for panels of industrial pavements heavily loaded. The results obtained are presented and analysed.

1 INTRODUCTION

The energy absorption capacity is the property most benefited by the addition of steel fibres to concrete [1]. Several methodologies have been proposed to evaluate the fracture toughness provided by fibre reinforcement [2-4], but none of them was accepted without reserves, and for each one several drawbacks were pointed out. The design practice of the structures having steel fibre reinforced concrete (SFRC) components requires the establishment of standard methods to characterize this composite material. To fit this purpose, RILEM designated a Technical Committee (TC 162-TDF) to develop standard bending test procedures, to propose parameters for characterizing the post-cracking behaviour, and to advance guidelines for designing SFRC structures under the framework of the Eurocode 2 [5-7]. Recently, this Committee published a document dealing with the concepts of the fracture mechanics for analysing the behaviour of the SFRC structures [8].

The present work is part of a research project where the main objectives were the development and the characterization of a cost competitive SFRC adjusted for industrial pavements, using the recommendations of the TC 162-TDF. The pre-requisites of such SFRC were the following:

- compression strength greater than 25MPa at 28 days;
- binding content, (Cement plus Fly Ash) equal to 300 kg/m^3;
- slump greater than 15 cm;
- materials available on the North Region of Portugal would be elected.

The experimental campaign carried out in this work had the main purpose of assessing the influence of the content of fibres (Cf), the age of the concrete (Ag) and the percentage of the cement replaced by fly ash (Fa) on the bending behaviour of the SFRC. To have a more deep understanding of the behaviour of the specimens, and to estimate the fibre reinforcement efficacy, the number and the distribution of the fibres on the fracture surface of the specimens were evaluated.

Slab specimens reinforced with steel fibres and conventional steel bars (mixed reinforcement) were also submitted to bending load configuration to characterize a reinforcement system adjusted for panels of industrial pavements heavily loaded.

The experimental tests are described, and the results obtained are presented and discussed.

2 RILEM RECOMMENDATIONS FOR SFRC

Figure 1 represents the standard test specimen recommended by RILEM TC 162-TDF [5, 9]. The production method for casting the specimen, the curing procedures, the position on the notch sawn into the test beam, the load and specimen support conditions, the characteristics for both the equipment and measuring devices, and the test procedures are given elsewhere [5, 9].

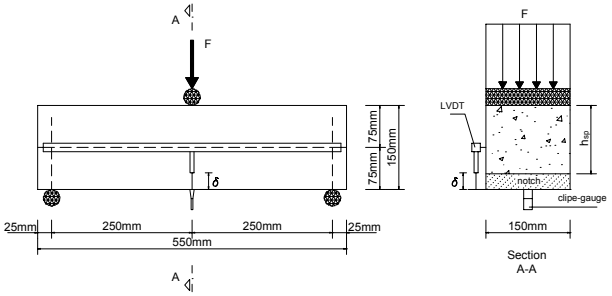

Figure 1: Specimen dimensions, arrangement of the displacement transducers and loading conditions

From a bending test it is obtained a force-deflection relationship (if a clip-gauge is mounted on the mouth of the notch, a force-crack mouth opening displacement relationship can also be registered). From this relationship it can be evaluated the load at the limit of proportionality (F_L) the equivalent flexural tensile strength parameters ($f_{eq,2}$ and $f_{eq,3}$) and the residual flexural tensile strength parameters ($f_{R,1}$ and $f_{R,4}$). F_L is equal to the highest value of the load registered up to a deflection of 0.05 mm. The parameters $f_{eq,2}$ and $f_{eq,3}$ are related to the energy absorption capacity up to a deflection of δ_2 and δ_3 ($\delta_2=\delta_L+0.65$mm, $\delta_3=\delta_L+2.65$mm were δ_L is the deflection correspondent to F_L) provided by fibre reinforcement mechanisms, ($D^f_{BZ,2}$ and $D^f_{BZ,3}$), see Figure 2 and Figure 3. The parameters $f_{R,1}$ and $f_{R,4}$ are the stresses due to forces $F_{R,1}$ and $F_{R,4}$, respectively, corresponding to a deflection of $\delta_{R,1}=0.46$mm and $\delta_{R,4}=3.0$ mm (see Figure 2 and Figure 3). The expressions for evaluating f_{eq} and f_R are inset on Figure 2 and Figure 3, where b (=150mm), h_{sp} (=125mm) and L (=500 mm) are the width of the specimen, the distance between the tip of the notch and the top of the cross section, and the span of the specimen, respectively. All these expressions were defined assuming a linear stress distribution on the cross section. According to RILEM TC 162-TDF [6] $f_{eq,2}$ or $f_{R,1}$ are used on the serviceability limit states while $f_{eq,3}$ or $f_{R,4}$ are taken on the ultimate limit states, under the framework of the Eurocode 2 [7].

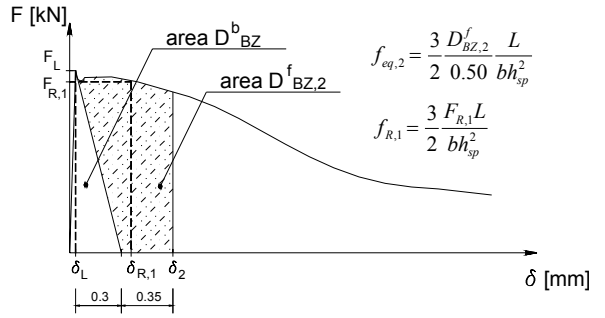

Figure 2: Evaluation of the equivalent two ($f_{eq,2}$) and residual one ($f_{R,1}$) flexural tensile strength parameters

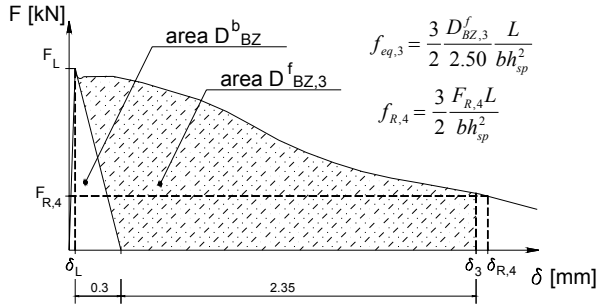

Figure 3: Evaluation of the equivalent three ($f_{eq,3}$) and residual four ($f_{R,4}$) flexural tensile strength parameters

3 MIX COMPOSITIONS

The first step of the present research was the development of a cost competitive SFRC for industrial pavements satisfying the following conditions: characteristic compression strength greater than 25MPa at 28 days; content of binding (cement + fly ash) equal to 300kg/m^3; slump greater than 15 cm; use of the aggregates available on the North Region of Portugal. Hooked ends DRAMIX® RC-80/60-BN steel fibres [10] were adopted since in previous works it was verified that this fibre can increase significantly the ultimate load bearing capacity of the concrete slabs on grade [11]. This fibre has a length (l_f) of 60mm, a diameter (d_f) of 0.75mm, an aspect ratio (l_f/d_f) of 80 and a yield stress of 1100MPa. The current content of fibres applied on industrial floors ranged from 10 to 35kg/m^3. Therefore, in the present experimental campaign it was designed compositions with 0, 10, 20 and 30kg/m^3 of fibres, described in Table 1, in order to perform an experimental characterization of concretes reinforced with representative fibre contents. It was decreased the water/cement ratio with the increment of fly ash, with the aim of obtaining a similar compression strength and mix workability in all compositions. This purpose was practically assured, as it is shown on Table 2. The influence of the fly ash was only appreciable at the age of 7 days. As it was expected, for the contents of fibres used, the influence of the fibres on the concrete compression strength was marginal [12]. A series of specimens was designated by FwCfjFaiAgk, where w is the type of fibre, j the content of fibres in kg/m^3, i the percentage of cement replaced by fly ash and k the age in days.

Component	Content [kg/m^3]		
Cement I 42.5R	300	262.5	225
Fly Ash	0 *(0%)*	37.5 *(12.5%)*	75 *(25%)*
Fine sand	173.5	165.5	152.3
Crushed sand	871.0	875.5	869.1
5/15 coarse aggregate	315.7	319.1	319.1
15/25 coarse aggregate	468.2	470.6	467
Water	163.8	158.8	153.8
Rheobuild® 1000	7.5		
Steel fibres (volume)	0 (0%); 10 *(0.12%)*; 20 *(0.25%)*; 30 *(0.38%)*		

Table 1: Mix compositions

Age [days]	Fly-ash [%]	Compression strength [MPa]
7	0	37,0
	12,5	30,1
	25	26,5
28	0	39,7
	12,5	39,3
	25	34,8
90	0	47,2
	12,5	46,6
	25	45,5

Table 2: Compression strength (evaluated on cubes of 150mm edge)

4 FIBRES DISPOSITION ON THE FRACTURE SURFACE

According to RILEM TC 162-TDF [5] the loading direction should be orthogonal to the casting direction. The SFRC designed in the present work has high workability, which can induce significant fibre

segregation during the compaction procedure. To evaluate the degree of the fibre segregation the fracture surface was discretized on four rows and five columns of cells, as it is represented in Figure 4. The average number of fibres counted was represented in Figure 5, where it can be observed an increment of the fibre percentage in the casting direction. This fibre segregation has promoted the development of non-uniform crack opening, as it is shown in Figure 6. Due to the lower percentage of fibres on the top surface in the casting direction, the crack in this surface was developed more quickly than on the bottom surface.

Therefore, for SFRC of high workability, placed with some vibration, fibre segregation has high probability to occur. To do a more realistic characterization of this type of SFRC, the loading direction and the casting direction should be the same.

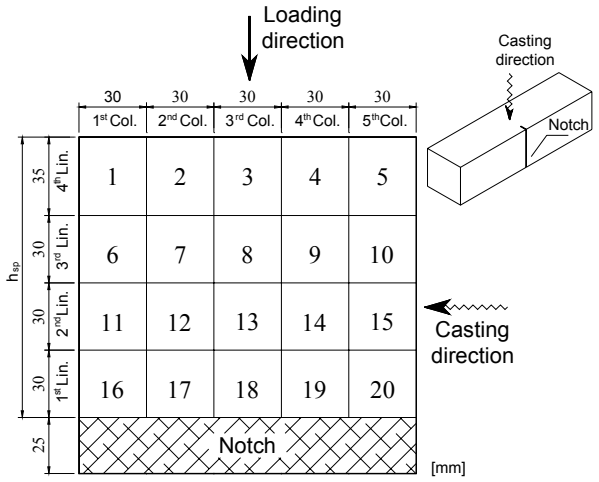

Figure 4: Specimen fracture surface discretized in cells

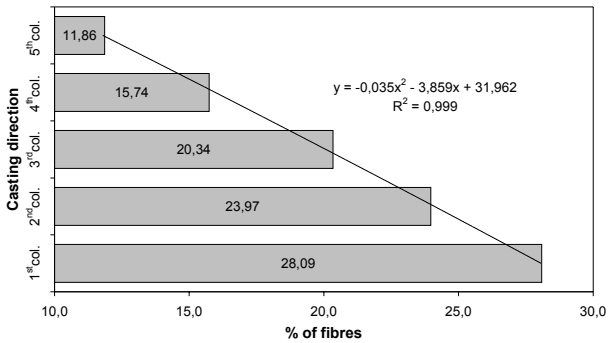

Figure 5: Average fibre distribution

5 RESULTS FROM THE BENDING TESTS

5.1 Introduction

In this section the results obtained on the bending tests carried out according to RILEM TC 162-TDF recommendations are presented in a format adjusted for showing, mainly, the influence of the fibre content.

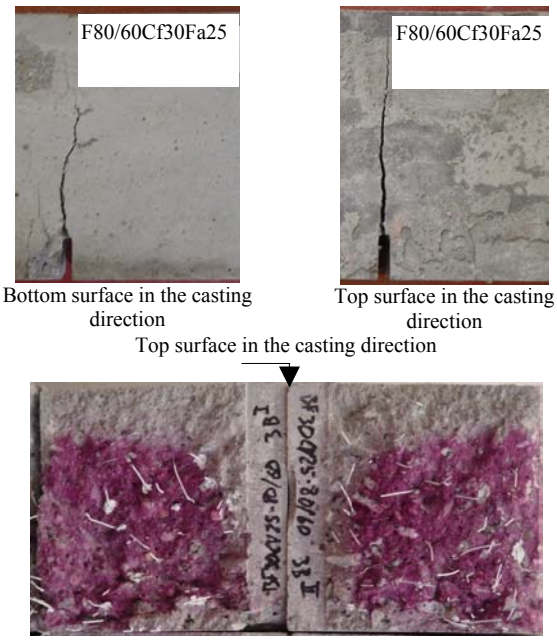

Figure 6: Non-uniform crack opening due to fibre segregation

5.2 Force-deflection relationships

The load-deflection relationship obtained on the specimens with the age of 7, 28 and 90 days is represented in Figures 7-9, respectively. Each curve is the average response of three specimens. From these relationships it can be pointed out the following observations:

- The residual strength (post peak load carrying capacity) increases with the fibre content;
- The fibre contribution is more relevant for the increment on the residual strength than for the increment on the peak load. In specimens F80/60Cf30Fa0Ag7, besides the residual strength, the peak load was also increased significantly. This was caused by the relative higher number of fibres found on the fracture surface of these specimens, but the quality of the fibre-matrix interface had also influence (lower quality for 25% of cement replacement by Fa);
- In some specimens, the residual strength has increased after peak load (hardening branch). This behaviour is associated to the occurrence of a higher concentration of fibres in the intermediate layers of the fracture surface. For instance, in specimens F80/60Cf30Fa0Ag7 the higher percentage of fibres has occurred in the second layer (2nd line of cells – see Figure 4), so the residual strength has increased when the reinforcement mechanisms of these fibres were activated, which happened for a deflection after peak load;
- The load decay just after the peak load appears to increase with the specimen age. This is caused by the increment of the concrete strength with its age, since higher energy is released when matrix cracks;
- After a deflection of about 0.7 mm the residual strength was maintained practically constant, indicating that $f_{eq,2}$ and $f_{eq,3}$ will have identical values, as well $f_{R,1}$ and $f_{R,4}$.

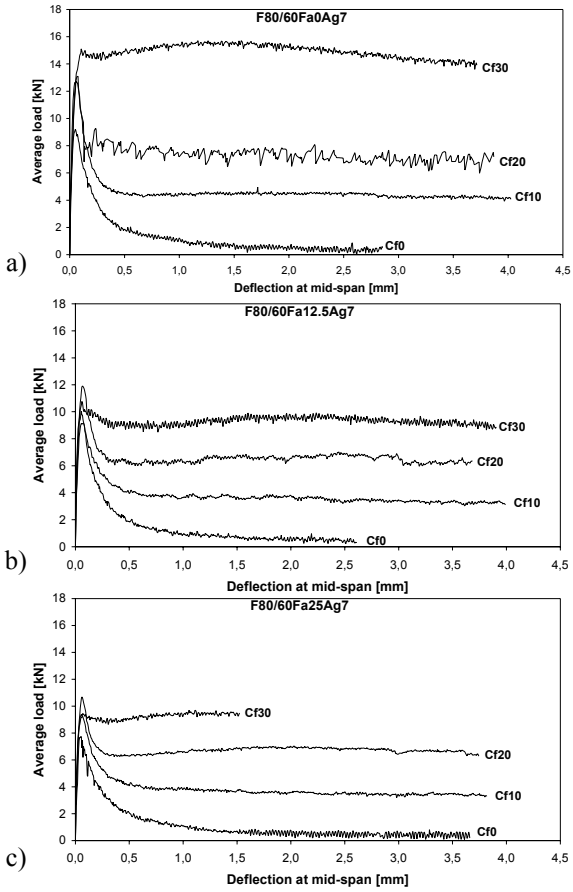

Figure 7: Force-deflection relationship on specimens with the age of 7 days: a) 0%; b) 12.5%; c) 25% of Fa

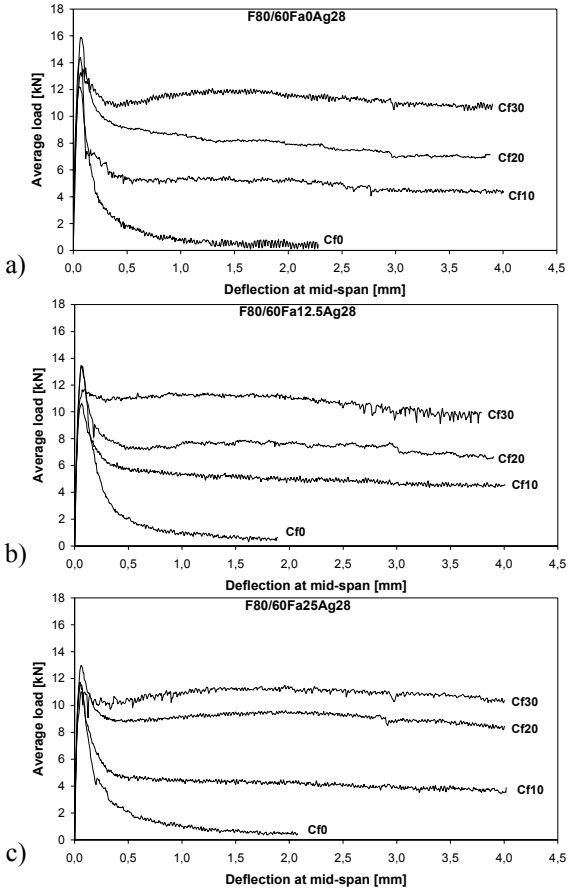

Figure 8: Force-deflection relationship on specimens with the age of 28 days: a) 0%; b) 12.5%; c) 25% of Fa

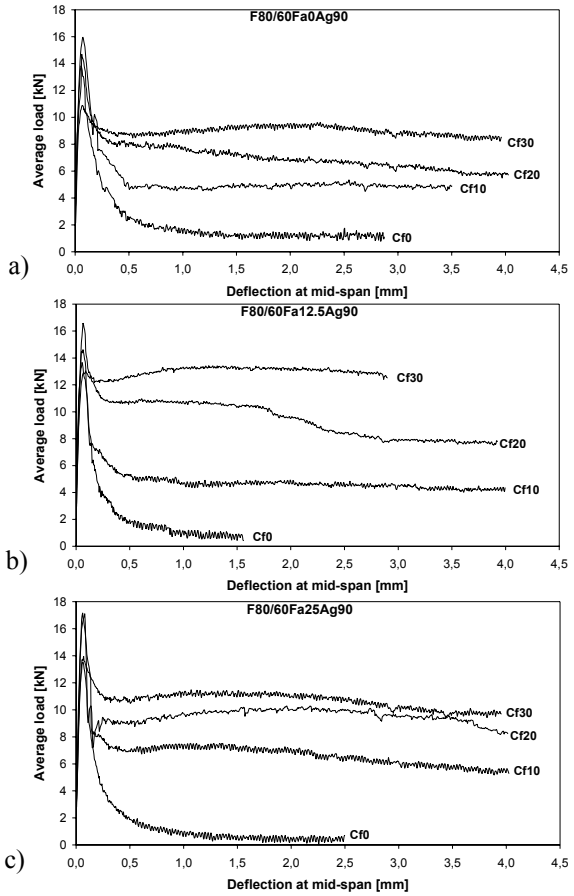

Figure 9: Force-deflection relationship on specimens with the age of 90 days: a) 0%; b) 12.5%; c) 25% of Fa

5.3 Equivalent flexural tensile strength parameters

The variation of the average values of $f_{eq,2}$ and $f_{eq,3}$ with the content of fibres (Cf) for the specimens with 7, 28 and 90 days is represented in Figures 10 and 11. From the curves depicted it is verified that, for the same age and content of fibres, $f_{eqm,2}$ and $f_{eqm,3}$ have similar values, revealing that the energy absorption capacity was maintained approximately constant up to the deflection of δ_3. Apart the specimens with 7 days, without Fa and with Cf above 20kg/m^3, in the remains $f_{eqm,2}$ and $f_{eqm,3}$ have an almost linear increment with Cf. In those specimens the increment of the $f_{eqm,2}$ and $f_{eqm,3}$ with Cf was higher. The number of fibres counted on the fracture surface of the series F80/60Fa0Ag7 and F80/60Fa12.5Ag7 was 88 and 61, which can justify this different increment ratio. However, the number of fibres evaluated on the fracture surface of the series F80/60Fa0Ag7 and F80/60Fa25Ag7 was quite similar (88 and 86) so, the higher increment on the f_{eq} registered on the series F80/60Fa0Ag7 might be related to the percentage of the cement replaced by Fa. For the age of 7 days this percentage of Fa might have decreased significantly the quality of the fibre-matrix interface, lowering the efficacy of the fibre reinforcement mechanisms. Comparing the results obtained at 28 days with the ones registered at 7 days it can be conclude that at 28 days f_{eqm} are not so affected by the presence of the Fa. At 90 days the specimens with 12.5% of Fa and with content of fibres greater than 10kg/m^3 have presented the highest values of f_{eqm}.

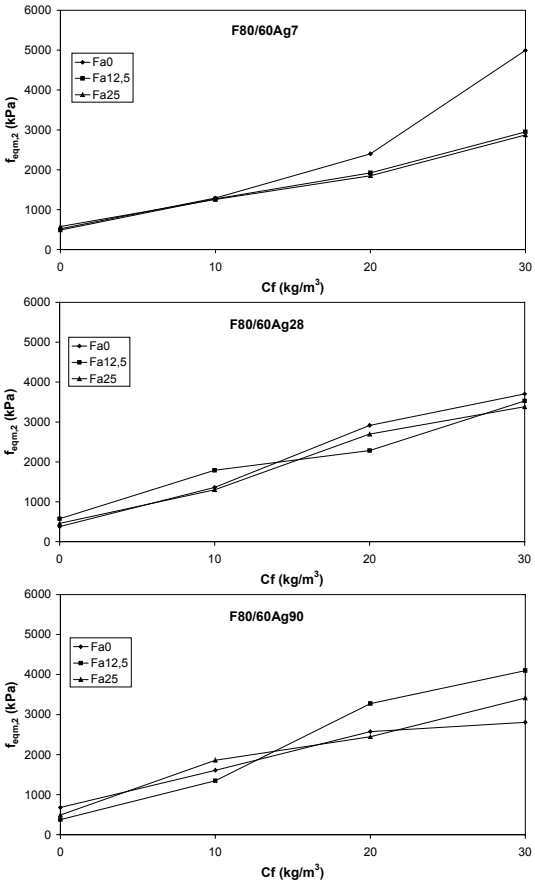

Figure 10: Relationship between $f_{eqm,2}$ and Cf for specimens with the age of 7 (a), 28 (b) a 90 (c) days

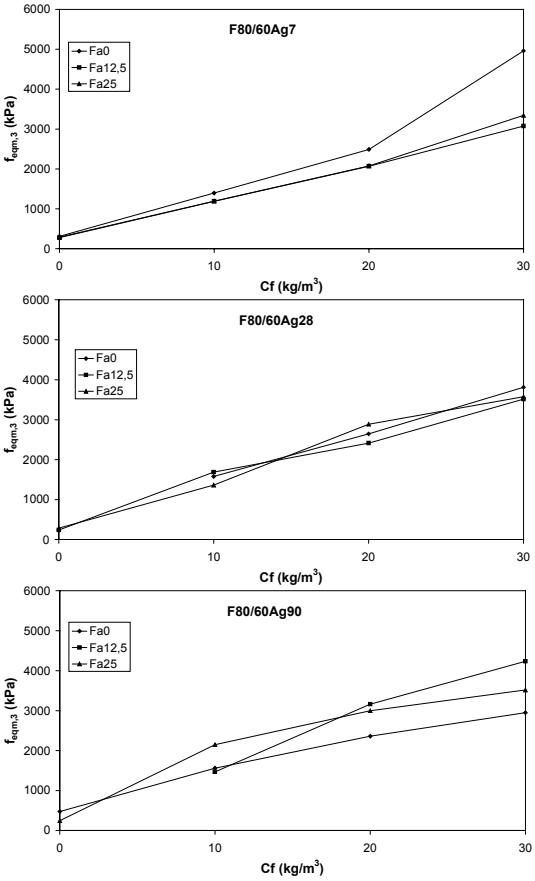

Figure 11: Relationship between $f_{eqm,3}$ and Cf for specimens with the age of 7 (a), 28 (b) a 90 (c) days

The relationship between $f_{eq,2}$ and $f_{R,1}$, and between $f_{eq,3}$ e $f_{R,4}$, are represented in Figure 12. It is observed a very good correlation between equivalent and residual flexural tensile strength parameters.

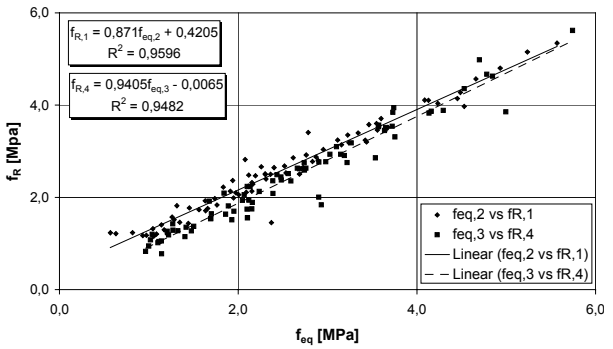

Figure 12: Relationships between equivalent and residual flexural tensile strength parameters

6 ASSESSING THE FIBRE REINFORCEMENT EFFICACY

The concrete compacting technique and the mould configuration are some of the factors that influence the fibre distribution into concrete. Due to the random character of the fibre distribution and the discrete fibre geometry, the efficacy of the fibre reinforcement is lower than the reinforcement provided by the conventional steel bars of equal cross section area. To take into account the length, the bond and the orientation of the fibres, some parameters were proposed to be used on the expression that predicts the post-cracking resistance of the SFRC [13].

To assess, in an indirect way, the fibre reinforcement efficacy of a given fibre distribution it was used a numerical model that takes into account the material constitutive laws, the equilibrium and the kinematics equations, and assumes that the RILEM specimen is divided into a non-linear hinge of length $h_{sp}/2$ (see Figures 1) where the main non-linear behaviour is concentrated, and into two other parts that are considered to behave elastically [8, 14]. To simulate the non-linear behaviour due to concrete cracking and to concrete inelastic deformation in compression, the cross section of the non-linear hinge was discretized on layers. This model gives the moment-curvature relationship of the cross section of the non-linear hinge and the force-deflection relationship of the specimen.

In the numerical simulation, the cross section of the non-linear hinge was discretized into 20 concrete layers and 4 strips of fictitious conventional reinforcement, SFCR, (see Figure 13). These strips were positioned on the middle of the four layers used for evaluating the number of fibres on the fracture surface (see Figure 4). The cross sectional area of the SFCR, A_{si}, was equal to the cross sectional area of the fibres found in the corresponding layer. The constitutive law attributed to the SFCR was defined from the values known for the steel fibres (Young's modulus of 200GPa and yield stress of 1100MPa). To characterize the concrete

compression constitutive law it was used the results obtained on the uniaxial compression tests. The concrete uniaxial tensile strength was evaluated from the corresponding compression strength, using the recommendations of the RILEM TC 162-TDF [5]. The fracture energy (G_f) the shape of the softening diagram and the width of the fracture process zone (l_b) were evaluated using the numerical model, fitting the force-deflection relationships registered on the plain concrete specimens. Using this approach the tensile stress-strain diagram represented in Figure 14 was obtained. Taking these fracture parameters in all the numerical simulations, and adopting for the compression and tensile strengths and for the cross section area of the SFCR the values observed experimentally, it was obtained the curves represented in Figures 15-17. The numerical simulations for all the series tested can be found elsewhere [15]. Analysing these results it is observed that the fibre reinforcement efficacy decreases with the increment of the fibre content, because the influence of the fibre-matrix bonding, the fibre length and the fibre orientation increases with the content of fibres. A load decay after the first peak load has occurred in all the numerical responses because the cross sectional area of the SFCR mobilized when concrete cracks was not enough to sustain the loss of load carrying capacity at this moment. For the specimens reinforced with 30kg/m^3 of fibres the numerical model predicted a significant load decay after the first peak load, which was not observed on the experimental responses. This behaviour can be due to the fact that steel fibres exist immediately above the tip of the notch, while in the numerical simulation the first SFCR was considered at 15mm above the tip of the notch.

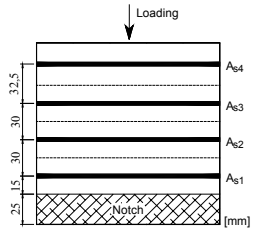

Figure 13 : Arrangement of the SFCR

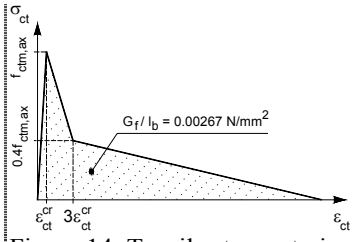

Figure 14: Tensile stress-strain diagram used on the numerical simulations

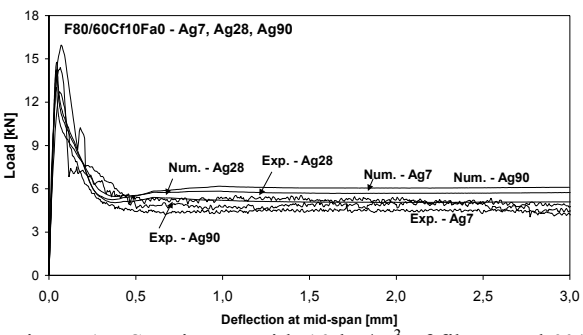

Figure 15: Specimens with 10 kg/m^3 of fibres and 0%Fa

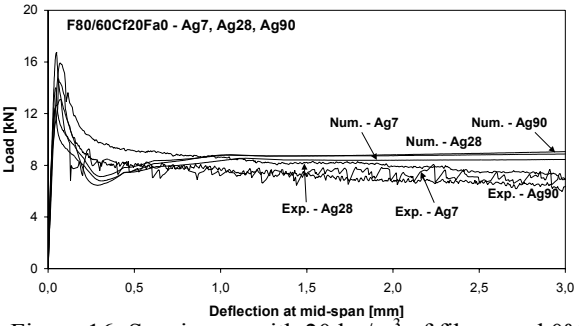

Figure 16: Specimens with 20 kg/m^3 of fibres and 0%Fa

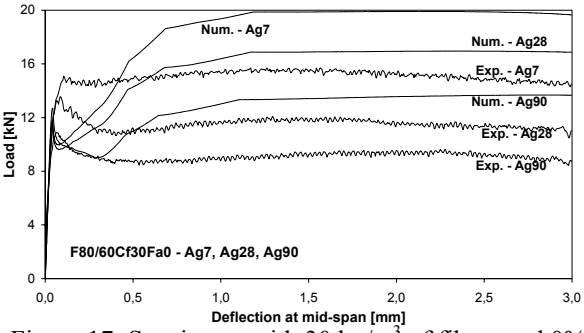

Figure 17: Specimens with 30 kg/m^3 of fibres and 0%Fa

7 MIXED REINFORCEMENT

7.1 Introduction

Usually, the design of an industrial pavement is done analysing one of the panels that it is composed. The maximum bending moment occurs when the loads actuate on the border of the panel, mainly, on the corner. The "non-linear lines" (yield lines according to the yield line theory [16, 17]) arise on the border of the panel and its distance to the panel contour depends on the slab and soil foundation rigidity [18]. Since the bending moments for the loads applied on the interior of the panel are much lower than the bending moments due to loads actuating on the panel contour, the design of the panel is conditioned by these last loading cases. Due to practical reasons, the concrete quality, the panel thickness, the reinforcement ratio, and the rigidity of the soil support are practically the same in the entire panel, i.e., the load bearing capacity is almost the same, in spite of the actuating moment is much higher in the border of the panel.

A much more rational design can be performed using a mixed reinforcement: steel fibres in the entire panel and a strip of conventional reinforcement (bars or grid mesh) placed on the contour of the panel. When well planed, this reinforcement arrangement does not introduce significant delays on the manufacture practice of an industrial floor. The content of the steel fibres is obtained in order to assure a resistant moment greater than the actuating moment developed due to the loads applied in the interior of the panel. The amount of conventional reinforcement placed in the panel contour should take the exceeding bending moment (difference between the bending moment due to the loads applied on the interior and on the contour of the panel).

To have results to enhance a numerical model that simulates the post cracking behaviour of concrete slab structures reinforced with conventional steel bars and steel fibres [19], a campaign of experimental tests was carried out. The results obtained on the specimens composing the first part of this campaign are presented and analysed on this section.

7.2 Materials and specimens

The concrete composition indicated in Table 1 (without fly ash) was used on the manufacturing the specimens tested. The specimens have a width of 300mm, a height of 80mm and a length of 650mm. Table 3 defines the series of tests carried out and the respective designation.

Content of fibres, Cf [kg/m^3]	Percentage of conventional reinforcement ratio, ρ_s		
	0	0.87	1.44
0	Cf0ρ_s0	Cf0ρ_s0.87	Cf0ρ_s1.44
20	Cf20ρ_s0	Cf20ρ_s0.87	Cf20ρ_s1.44
40	Cf40ρ_s0	Cf40ρ_s0.87	Cf40ρ_s1.44

Table 3: Series of tests

Table 4 includes the average compression strength and the respective standard deviation (in brackets) registered on the series of different content of fibres, at 28 days. Each value is the average of four tests with cylinder specimens (150mm diameter and 300mm height). In these tests the increment of the concrete compression strength with the increment of fibre content was not marginal.

	Content of fibres [kg/m^3]		
	0	20	40
f_{cm} [MPa]	28.40 (7.38)	32.00 (6.59)	38.87 (5.86)

Table 4: Average Uniaxial compression strength.

The campaign was composed by a total of nine series of tests, each one having three specimens. To evaluate the influence of the fibre content it was produced three series with different content of fibres (Cf): 0, 20 and 40kg/m^3 of hooked ends DRAMIX® RC-80/60-BN steel fibres. To assess the influence of the percentage of the conventional reinforcement, each one of aforementioned series is composed by three sub-series of different percentage of longitudinal conventional reinforcement ratio (ρ_s): 0, 0.87 and 1.44. This percentage was determined according to the recommendations of the CEB-FIP Model Code 1993 [20]. Figure 18 represents the reinforcement arrangements adopted.

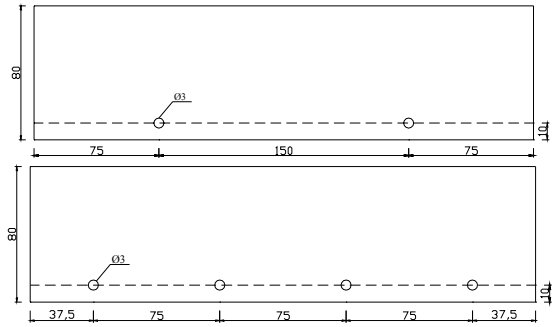

Figure 18: Reinforcement arrangements (units in mm)

Figure 19 depicts the stress-strain relationships registered on uniaxial tensile tests carried out with three specimens of conventional reinforcement.

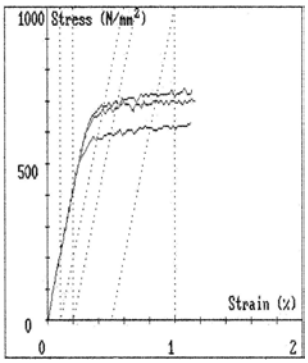

Figure 19: Stress-strain relationship of the conventional reinforcement

7.3 Test set-up and test procedures

Figure 20 illustrates the test set-up adopted. Five LVDTs supported on a Japanese yoke system (JYS) [1] were used for evaluating the deformation of the specimen. The JYS was used to avoid the register of the extraneous displacements. In spite of this caution, parasitic displacements can be measured if the specimen was submitted to large deformations because, in this case, the points where the JYS are attached to the specimen can have some movements [1]. To take into account these movements two LVDTs were placed on these points.

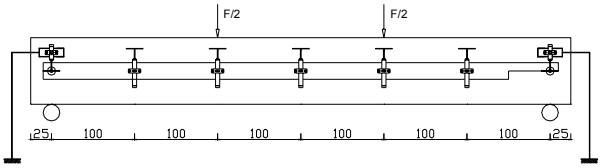

Figure 20: Arrangement of measuring devices and loading configuration

The specimens were submitted to four line loads. The tests were controlled by the deflection measured at the LVDT placed at specimen mid-span, using a displacement ratio of 0.6mm/min. The forces were measured from a load cell of 250kN load bearing capacity and ± 0.05% of linearity.

7.4 Results

Figure 21 and Figure 22 represents the variation of the maximum load with the fibre content (Cf) and with the reinforcement ratio (ρ_s), respectively. From these figures it can be verified that the maximum load is only increased for content of fibres above 20 kg/m^3, while increasing ρ_s the maximum load increases almost linearly.

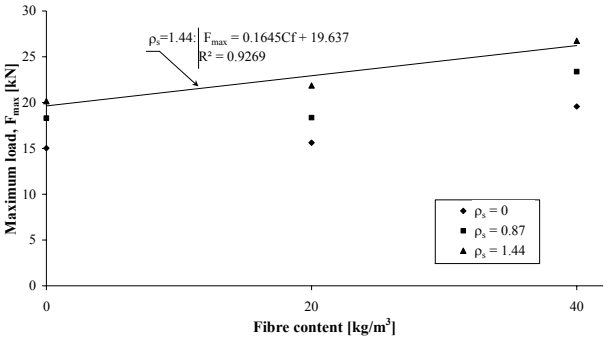

Figure 21: Variation of the maximum load with the fibre content

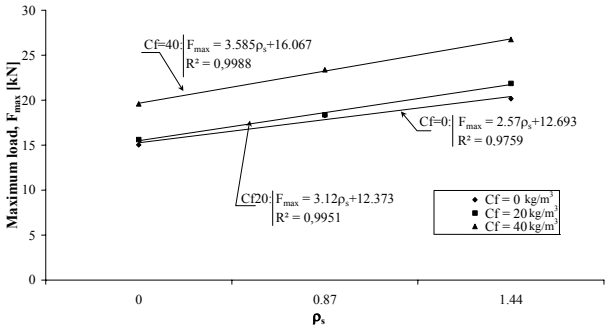

Figure 22: Variation of the maximum load with the longitudinal reinforcement ratio

To evaluate the effect of the mixed reinforcement on the material energy absorption capacity it was determined the equivalent flexural tensile strength up to a deflection of δ_2 ($f_{eq,\delta 2}$) and δ_3 ($f_{eq,\delta 3}$), using the procedures and the assumptions described on section 2. Figure 23 and Figure 24 represent the variation of the $f_{eq,\delta 2}$ with the Cf and ρ_s, respectively, while Figure 25 and Figure 26 depicts the variation of the $f_{eq,\delta 2}$ with these same parameters. From these Figures it can be observed that $f_{eq,\delta 2}$ and $f_{eq,\delta 3}$ increase with Cf, mainly above 20kg/m^3 of fibres. For the Cf and ρ_s used, and when Cf>0kg/m^3, the increase of the $f_{eq,\delta 2}$ and $f_{eq,\delta 3}$ with ρ_s appears to tend for an asymptote, showing that, for increasing the concrete energy absorption capacity the fibres are more effective than the conventional reinforcement. Figure 23 and Figure 25 reveal that above 20kg/m^3 of fibres the increase of the $f_{eq,\delta 2}$ and $f_{eq,\delta 3}$ is so much higher as smaller is the conventional reinforcement ratio.

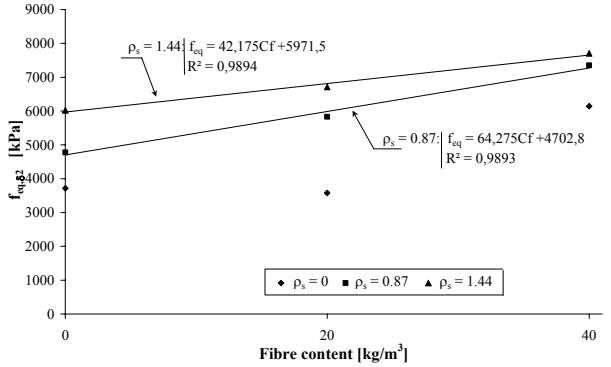

Figure 23: Variation of the $f_{eq,\delta 2}$ with the fibre content

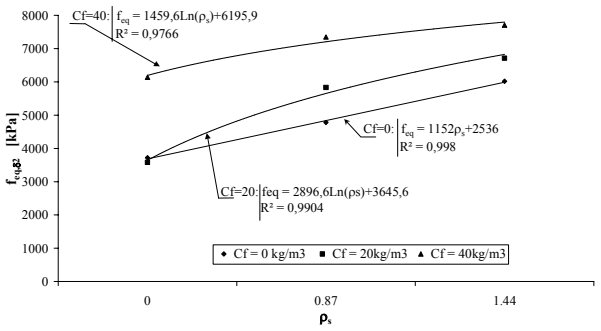

Figure 24: Variation of the $f_{eq,\delta 2}$ with the conventional reinforcement ratio

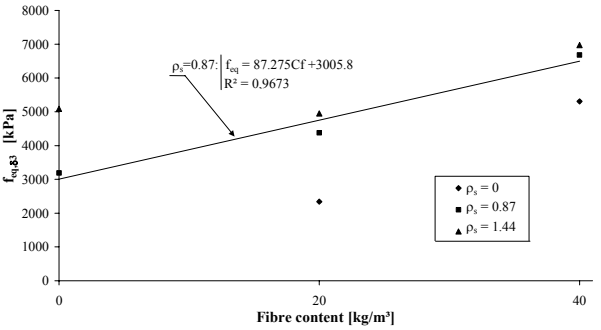

Figure 25: Variation of the $f_{eq,\delta 3}$ with the fibre content

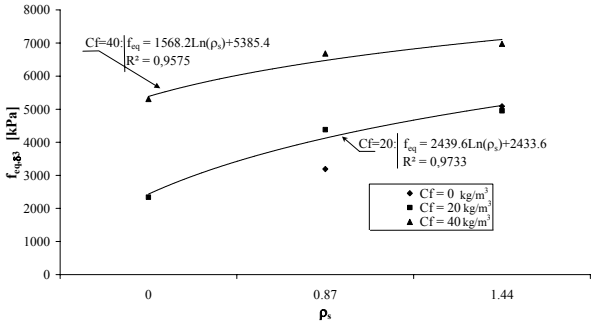

Figure 26: Variation of the $f_{eq,\delta 3}$ with the conventional reinforcement ratio

8 CONCLUSIONS

In the present work the bending behaviour of a cost competitive steel fibre reinforced concrete (SFRC) for industrial pavements was experimentally characterized according to the most recent recommendations of RILEM TC 162-TDF Committee. The SFRC developed has enough compression strength and workability for this kind of application. In its production the binding (cement + fly ash) was maintained equal to 300kg/m^3 and local aggregates, not treated, were used. Increasing the percentage of replacement of cement by fly ash, the water/cement ratio was decreased in order to assure more economical compositions with similar compression strength and workability.

The SFRC compositions developed had a slump greater than 15 cm, and the bending specimens were compacted on a current vibrating table. A linear increase of the fibre percentage on the casting direction was observed,

revealing that, for compositions with high workability (the necessary for pavements applications), placed with some vibration, fibre segregation occurs. In this case, for getting a realistic experimental characterization of the bending behaviour of this SFRC, the loading should have the direction of the concrete casting. In industrial floors practice, the SFRC has high workability and are placed with reduced or null external vibration. To characterize the bending behaviour of this SFRC, the specimens should be compacted with similar vibration energy.

From the bending tests carried out according to TC 162-TDF recommendations it was verified that:

- the force-deflection post-peak behaviour is conditioned by the fibre distribution of the fracture surface of the specimen. The energy absorption capacity, used on the determination of the equivalent flexural tensile strength parameters proposed by TC 162-TDF ($f_{eq,2}$, $f_{eq,3}$), is too dependent on the number of fibres on the fracture surface, while the fibre distribution on the fracture surface influences the shape of the post-peak response. An abnormal concentration of fibres in a given intermediate layer of the specimen fracture surface can induce a "hardening" branch on the post-peak of the load-deflection relationship;
- for the SFRC developed it was verified that $f_{eq,2}$ and $f_{eq,3}$ have similar values, revealing that the energy absorption capacity was maintained almost constant up to a deflection of ≈2.7mm, the deflection adopted for evaluating $f_{eq,3}$, used on the ultimate limit state verifications;
- in specimens with 28 days the f_{eq} are not affected by the presence fly ash, Fa, (a maximum percentage of 25% of cement was replaced by fly ash). At 90 days specimens with 12.5% of cement replaced by Fa and with content of fibres greater than 10kg/m^3 have presented the highest values of f_{eq};
- a very good correlation between equivalent (f_{eq}) and residual (f_R) flexural tensile strength parameters was achieved;

In order to assess the fibre reinforcement efficacy, the number and the distribution of the fibres counted on the fracture surface of the specimens tested were used for proposing a fictitious conventional reinforcement of a cross sectional area equal to these fibres. Using a numerical model that takes into account the material constitutive laws, the equilibrium and kinematic equations, and assumes that the non-linear behaviour is concentrated in a non-linear hinge placed at specimen centre, it was concluded from comparing the experimental and the numerical responses, that the fibre reinforcement efficacy decreases with the increment of the fibre content.

To develop a more rational reinforcement system for heavily loaded industrial pavements, it was carried out four point bending tests with slab specimens reinforced with different content of fibres and conventional reinforcement ratio (mixed reinforcement). From the main results it was verified:

- the maximum load is only increased for content of fibres above 20kg/m^3, while increasing the reinforcement ratio the maximum load increases almost linearly;
- the equivalent flexural tensile strength parameters increased with the content of fibres, mainly above 20kg/m^3. In the specimens reinforced with fibres, the increment of these parameters with the reinforcement ratio has tended for an asymptote, showing that, for increasing the concrete energy absorption capacity, the fibres are more effective than the conventional reinforcement.

ACKNOWLEDGEMENTS

The study reported in this paper forms a part of the research program "Cost competitive steel fibre reinforced concrete for industrial pavements " supported by FCT, POCTI/34793/99. The aggregates were generously supplied by "Pisonort – Pavimentos industriais Lda", the cement by Secil, the superplasticizer by MBT, the fly ash by "Central do Pego" and the fibres by Bekaert NV. Special thanks for Civitest Lda for the lending of some test equipment.

REFERENCES

[1] Barros, J.A.O.: Sena Cruz, J.M: Fracture energy of steel fibre reinforced concrete. Journal of Mechanics of Composite Materials and Structures, Vol. 8, No. 1, pp.29-45, January-March 2001.

[2] Gopalaratnam, V.S. et al.: Fracture toughness of fiber reinforced concrete. ACI Materials Journal, Vol. 88, Nº. 4, pp. 339-353, July-August 1991.

[3] Balaguru, P.N.: Shah, S.P.: Fiber reinforced cement composites. McGraw-Hill International Editions, Civil Engineering Series, 1992.

[4] ACI 544.1R-96: State-of-the-Art Report on Fiber Reinforced Concrete. ACI, 1997.

[5] RILEM TC 162-TDF Committee: RILEM 162-TDF: Test and design methods for steel fibre reinforced concrete. Materials and Structures, Vol. 33, pp 3-5 January-February 2000a.

[6] RILEM TC 162-TDF Committee: RILEM 162-TDF: Test and design methods for steel fibre reinforced concrete. Materials and Structures, Vol. 33, pp 75-81, March 2000b.

[7] European pre-standard: ENV 1992-1-1: Eurocode 2: Design of concrete structures – Part 1: General rules and rules for buildings.

[8] RILEM TC 162-TDF Committee: RILEM 162-TDF: Test and design methods for steel fibre reinforced concrete. Materials and Structures, Vol. 35, pp. 262-278, June 2002.

[9] RILEM TC 162-TDF: Test and Design Methods for Steel Fibre Reinforced Concrete. Recommendations (work document), 05 February 2002.

[10] Dramix: Product data sheet, N.V.Bekaert S.A., 1998.

[11] Barros, J.A.O.: Figueiras, J.A.: Experimental behaviour of fiber concrete slabs on soil. Journal Mechanics of Cohesive-frictional Materials, Vol. 3, pp. 277-290, 1998.

[12] Barros, J.A.O.: Antunes, J.A.B: Amorim, J.A.S.B.A.: Influência da quantidade de fibras, percentagem de cinzas volantes e idade no comportamento à flexão de betão reforçado com fibras de aço Dramix RC-80/60-BN (Influence of the content of fibres, percentage of fly ash and concrete age on the bending behaviour of concrete reinforced with Dramix RC-80/60-BN steel fibres). Repport 02-DEC/E-11, 87 pp., July 2002. (in Portuguese)

[13] Lim, T.Y.: Paramasivam, P.: Lee, S.L.: Analytical model for tensile behavior of steel-fiber concrete. ACI Materials Journal, pp. 286-298, July-August 1987.

[14] Barros, J.A.O.: Figueiras, J.A.: Flexural behavior of steel fiber reinforced concrete: testing and modelling. Journal of Materials in Civil Engineering, ASCE, Vol. 11, Nº 4, pp 331-339, 1999.

[15] Barros, J.A.O.: Antunes, J.A.B.: Amorim, J.A.S.B.A.: Eficácia de fibras discretas de aço no reforço à flexão de elementos de betão (Efficacy of the discrete fibres on the concrete bending reinforcement). Congresso Nacional da Engenharia de Estruturas, LNEC, Lisboa, pp. 283-292, 10-13 July 2002. (in Portuguese)

[16] Losberg, A.: Design methods for structurally reinforced concrete pavements. Transactions of Chalmers University of Technology Gothenburg, Sweden, 1961.

[17] Baumann, R.A.: Weisgerber, F.E.: Yield line analysis of slabs-on-grade. Jour. Struct. Engrg. ASCE, 1983, 109(7), 1553-1568.

[18] Barros, J.A.O.: Analysis of concrete slabs supported on soil. IV Congreso Métodos Numéricos en Ingeniería, SEMNI, Sevilha, June 1999. (invited paper)

[19] Barros, J.A.O.: Comportamento do betão reforçado com fibras - análise experimental e simulação numérica (Behaviour of fibre reinforced concrete – experimental analysis and numerical simulation). PhD Thesis, Civil Eng. Dept., Faculty of Engineering, University of Porto, Portugal, 1995. (in Portuguese).

[20] CEB-FIP Model Code: Design code. Bulletin d'Information CEB Lausanne, Switzerland, 1993.